Available online at www.sciencedirect.com
ScienceDirect
Journal of Sound and Vibration 306 (2007) 908–927
JOURNAL OF SOUND AND VIBRATION
www.elsevier.com/locate/jsvi

An analytical method for the in-plane vibration analysis of rectangular plates with elastically restrained edges

Jingtao Du[a,*], Wen L. Li[b], Guoyong Jin[a], Tiejun Yang[a], Zhigang Liu[a]

[a]*College of Power and Energy Engineering, Harbin Engineering University, Harbin 150001, PR China*
[b]*Department of Mechanical Engineering, Wayne State University, 5050 Anthony Wayne Drive, Detroit, MI 48202-3902, USA*

Received 6 March 2007; received in revised form 29 May 2007; accepted 30 June 2007

Abstract

In this investigation, the in-plane vibration problems are solved for plates with general elastically restrained boundary conditions. Under the current framework, all the classical homogeneous boundary condition for in-plane displacements can be easily simulated by simply setting the stiffnesses of the restraining springs to either infinite or zero. The vibration problems are solved using an improved Fourier series method in which the in-plane displacements are expressed as the superposition of a double Fourier cosine series and four supplementary functions in the form of the product of a polynomial function and a single cosine series expansion. The use of these supplementary functions is to overcome the discontinuity problems which the original displacement functions will potentially encounter along the edges when they are viewed as a periodic function defined over the entire x–y plane. The excellent accuracy and convergence of the current solution are demonstrated through numerical examples. To the best of authors' knowledge, this work represents the first time that an analytical solution has been obtained for the in-plane vibrations of a rectangular plate with elastically restrained edges.

1. Introduction

It is well known that a vibrating flat plate can exhibit three types of waveforms: bending, longitudinal and shear. Of these three wave groups, bending is often referred to as the out-of-plane vibration, and longitudinal and shear waves as the in-plane vibrations [1]. The transverse bending vibrations of plates have received much attention in the literature, and a huge amount of results have been published regarding the vibrations and modal characteristics of plates with various structural features and/or boundary conditions [2,3]. Probably because of the fact that the modes related to in-plane vibrations typically fall outside the dominant frequency bands of excitations, the in-plane vibration problems are far less studied as evidenced by few publications available in the literature. In certain engineering applications, however, the in-plane and flexural vibrations need to be taken into consideration altogether. Some studies have shown that in-plane

*Corresponding author. Tel.: +86 451 82518264; fax: +86 451 82569458.
E-mail address: jingtaodu828@yahoo.com.cn (J. Du).

0022-460X/$ - see front matter © 2007 Elsevier Ltd. All rights reserved.
doi:10.1016/j.jsv.2007.06.011

Nomenclature

a	length of a plate
b	width of a plate
c_L	longitudinal wave speed in the plate ($c_L = \sqrt{E/\rho(1-\mu^2)}$)
E	Young's modulus
k	stiffness of the restraining springs
$\mathbf{K}$	stiffness matrix
$\overline{K}$	non-dimensional stiffness ($\overline{K} = ka(1-\mu^2)/E$)
$\mathbf{M}$	mass matrix
r_1	plate aspect ratio ($r_1 = a/b$)
r_2	inverse of plate aspect ratio ($r_2 = b/a$)
$u(x,y)$	in-plane displacement component in the x-direction
$v(x,y)$	in-plane displacement component in the y-direction
δ_{mn}	Kronecher delta function
λ_{am}	($\lambda_{am} = m\pi/a$)
λ_{bn}	($\lambda_{bn} = n\pi/b$)
μ	Poisson's ratio
ρ	mass density of plate material
σ_x,σ_y	in-plane normal stresses
τ_{xy}	in-plane shear stress
ω	angular frequency
Ω	dimensionless frequency ($\Omega = \omega a\sqrt{\rho(1-\mu^2)/E}$)

vibrations can play a major role for the transmissions of high-frequency vibration energies in build-up structures [1,4,5]. However, the importance of in-plane vibrations should not be only understood in context of the high-frequency vibrations or energy transmissions; they can meaningfully affect the low-frequency vibrations as well. When two plates are connected at an angle along an edge, the in-plane and out-of-plane displacements are directly coupled together in the form of kinematic constraints and/or kinetic equations. Although the coupling terms may be of secondary interest and usually ignored in the governing differential equations, the same cannot be said about them in regards to the boundary condition equations. For instance, when two plates are connected together perpendicularly, the substantial resistance to both flexural deflections at the junction cannot be properly captured without considering the in-plane modes even though their natural frequencies are outside (or far above) the frequency range of concern. There can also be a direct correlation between the in-plane vibrations and the noise radiated into the immediate environment [6]. The in-plane vibrations may also have an important implication to the non-destructive evaluation of the model parameters and failure modes of composite and sandwich plates as will be explained later.

Most existing studies on the free in-plane vibrations of rectangular plates are limited to the classical homogeneous boundary conditions. To the best of authors' knowledge, there is no work reported in the open literature about the free in-plane vibrations of rectangular plates with elastically restrained edges. Recently, Li [7] proposed a Fourier series method for the vibration analysis of arbitrarily supported beams. The flexural displacement of the beam is sought as the linear combination of a Fourier series and an auxiliary polynomial function. Subsequently, this method is extended to the flexural vibrations of rectangular plates under general boundary conditions [8]. It has been shown that this solution method works very well for plates with various edge supports.

The objective of this investigation is to extend the aforementioned Fourier series method to the in-plane vibrations of rectangular plates with general elastically restrained edges. From solution point of view, the current method is meaningfully different from the previous ones in that the plate displacements now exactly satisfy both the governing differential equations and the boundary conditions, rather than in a weak (variational) sense as the Rayleigh-Ritz solutions do. Theoretically, this notion is of fundamental importance because it has been widely accepted that there is no exact solution for a rectangular plate with general boundary conditions. Another significant distinction is that the in-plane wave field involves two coupled displacement variables in contrast to the flexural field described only by one single variable, thus leading to a more complicated boundary value problem to solve. Sufficient details are presented regarding how the solution is derived for a rectangular plate with elastically restrained edges. Finally, several numerical examples are solved to demonstrate the excellent accuracy and convergence of the current solution.

2. Theoretical formulations

2.1. Boundary conditions for an elastically restrained plate

In the study of transverse vibration of a thin rectangular plate, the general boundary conditions can be specified in terms of two kinds of springs (rotational and linear springs) attached to each edge. As a result, all the classical boundary conditions can be readily obtained by accordingly setting the spring constants equal to an extremely large or small number [8]. Similarly, the general boundary conditions for the in-plane displacements can be represented by two sets of linear springs along each edge, as illustrated in Fig. 1. When the stiffness for both sets of springs along an edge becomes infinitely large, that edge is essentially clamped. The free edge condition can be simply obtained by setting stiffnesses for these two sets springs to zero. There are two types of simply supported boundary conditions for the in-plane vibration problems. One is that on a given edge the displacement parallel to it is fully restrained while the normal displacement is completely free, which is equivalent to specifying the infinite stiffness for the tangential springs, and zero stiffness for the normal springs. The other represents an opposite situation involving infinitely rigid normal springs, and extremely soft tangential springs. These two edge conditions are referred to as the first type (SS1) and the second type (SS2) simply supported boundary conditions [6], respectively.

According to the plane stress theory in elasticity, the normal and shear stresses can be written as

$$\sigma_x = \frac{E}{1-\mu^2}\left(\frac{\partial u}{\partial x} + \mu\frac{\partial v}{\partial y}\right), \tag{1}$$

$$\sigma_y = \frac{E}{1-\mu^2}\left(\mu\frac{\partial u}{\partial x} + \frac{\partial v}{\partial y}\right) \tag{2}$$

and

$$\tau_{xy} = \frac{E}{1-\mu^2}\frac{1-\mu}{2}\left(\frac{\partial u}{\partial y} + \frac{\partial v}{\partial x}\right), \tag{3}$$

where u and v are the in-plane displacements in the x- and y-direction, respectively; E and μ are the Young's modulus and Poisson's ratio of the plate material, respectively (a list of symbols is given in the Nomenclature).

The boundary conditions for elastically restrained edges are as follows:

$$\overline{k}_{nx0}u = \frac{\partial u}{\partial x} + \mu\frac{\partial v}{\partial y}, \quad K_{px0}v = \frac{\partial u}{\partial y} + \frac{\partial v}{\partial x} \quad \text{at } x = 0, \tag{4,5}$$

$$\overline{k}_{nx1}u = -\left(\frac{\partial u}{\partial x} + \mu\frac{\partial v}{\partial y}\right), \quad K_{px1}v = -\left(\frac{\partial u}{\partial y} + \frac{\partial v}{\partial x}\right) \quad \text{at } x = a, \tag{6,7}$$

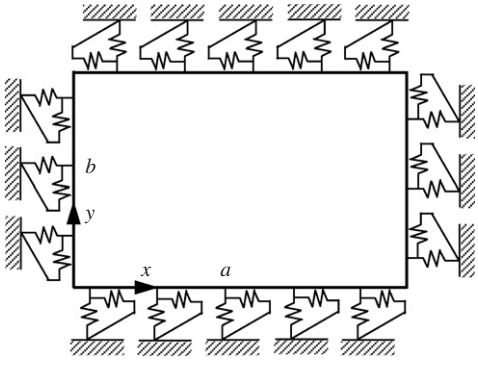

Fig. 1. A rectangular plate with elastic edge supports for in-plane vibration.

$$\overline{k}_{ny0}v = \mu\frac{\partial u}{\partial x} + \frac{\partial v}{\partial y}, \quad K_{py0}u = \frac{\partial u}{\partial y} + \frac{\partial v}{\partial x} \quad \text{at } y = 0 \tag{8,9}$$

and

$$\overline{k}_{ny1}v = -\left(\mu\frac{\partial u}{\partial x} + \frac{\partial v}{\partial y}\right), \quad K_{py1}u = -\left(\frac{\partial u}{\partial y} + \frac{\partial v}{\partial x}\right) \quad \text{at } y = b, \tag{10,11}$$

where $\overline{k} = k(1-\mu^2)/E$ and $K = 2\overline{k}/(1-\mu)$ with k being the stiffness of the restraining springs. The subscripts with $\bar{k}$ and K indicate the direction and location of the corresponding springs. For example, k_{nx0} and k_{px1} present the stiffness for the normal springs along the edge $x = 0$ and the stiffness for the tangential springs at $x = a$, respectively. As mentioned earlier, all classical homogeneous boundary conditions can be easily derived by simply setting each of the spring stiffnesses to be an extremely large or small number.

For in-plane vibration problems, there involve two independent field variables which can be conveniently chosen as the displacements in x- and y-direction. In this study, these displacements are expressed in form of Fourier series expansions:

$$\begin{aligned} u(x,y) = & \sum_{m=0}^{\infty}\sum_{n=0}^{\infty} A_{mn}\cos\lambda_{am}x\cos\lambda_{bn}y \\ & + \xi_{1b}(y)\sum_{m=0}^{\infty} a_m\cos\lambda_{am}x + \xi_{2b}(y)\sum_{m=0}^{\infty} b_m\cos\lambda_{am}x \\ & + \xi_{1a}(x)\sum_{n=0}^{\infty} c_n\cos\lambda_{bn}y + \xi_{2a}(x)\sum_{n=0}^{\infty} d_n\cos\lambda_{bn}y \end{aligned} \tag{12}$$

and

$$\begin{aligned} v(x,y) = & \sum_{m=0}^{\infty}\sum_{n=0}^{\infty} B_{mn}\cos\lambda_{am}x\cos\lambda_{bn}y \\ & + \xi_{1b}(y)\sum_{m=0}^{\infty} e_m\cos\lambda_{am}x + \xi_{2b}(y)\sum_{m=0}^{\infty} f_m\cos\lambda_{am}x \\ & + \xi_{1a}(x)\sum_{n=0}^{\infty} g_n\cos\lambda_{bn}y + \xi_{2a}(x)\sum_{n=0}^{\infty} h_n\cos\lambda_{bn}y, \end{aligned} \tag{13}$$

where $\lambda_{am} = m\pi/a$, $\lambda_{bn} = n\pi/b$, and

$$\xi_{1a}(x) = a\zeta_x(\zeta_x - 1)^2, \quad \xi_{2a}(x) = a\zeta_x^2(\zeta_x - 1) \quad (\zeta_x = x/a), \tag{14a,b}$$

$$\xi_{1b}(y) = b\zeta_y(\zeta_y - 1)^2 \text{ and } \xi_{2b}(y) = b\zeta_y^2(\zeta_y - 1) \quad (\zeta_y = y/b). \tag{15a,b}$$

It is easy to verify that

$$\xi_{1a}(0) = \xi_{1a}(a) = \xi'_{1a}(a) = 0, \quad \xi'_{1a}(0) = 1, \tag{16a,b}$$

$$\xi_{2a}(0) = \xi_{2a}(a) = \xi'_{2a}(0) = 0, \quad \xi'_{2a}(a) = 1. \tag{17a,b}$$

Similar conditions exist for the y-related polynomials, $\xi_{1b}(y)$ and $\xi_{2b}(y)$. It should be noted that the satisfaction of Eqs. (16) and (17) is not inherently required by the current method; such conditions are imposed purely for the sake of simplifying the subsequent mathematical expressions and the corresponding solution procedures. For instance, as easily seen from Eq. (18), the number of terms can be significantly reduced in the final representations of the boundary conditions.

One shall notice from Eqs. (12) and (13) that besides the standard double Fourier series defined over the domain R^2:((0,a)⊗(0,b)), four single Fourier series are also included in each of the displacement expressions. In light of Eqs. (16a) and (16b), it is not difficult to see that the fourth term (or the third single Fourier series term) on the right-side of Eq. (12) is actually equal to the derivative (with respect to x) of the displacement function $u(x,y)$ at edge $x = 0$. In other words, the potential discontinuity (or jump) associated with the

x-derivative of the original displacement $u(x,y)$ at $x = 0$ is effectively transferred onto the supplementary term. As a result, the residual displacement represented by the double Fourier series expansion is guaranteed to have a continuous derivative across the edge $x = 0$ when it is periodically extended onto the entire x-axis. In the same way, three additional single Fourier terms are introduced to deal with the possible derivative jumps along the other three edges. Therefore, not only is this Fourier series representation of solution applicable to any boundary conditions, but also the convergence of the series expansion can be substantially improved and guaranteed to a speed of, at least, $(m\pi)^3$.

Substituting Eqs. (12) and (13) into the boundary conditions, for example, at $x = 0$, one will have

$$\overline{k}_{nx0}\left(\sum_{m=0}^{\infty}\sum_{n=0}^{\infty}A_{mn}\cos\lambda_{bn}y+\xi_{1b}(y)\sum_{m=0}^{\infty}a_m+\xi_{2b}(y)\sum_{m=0}^{\infty}b_m\right)$$
$$=\sum_{n=0}^{\infty}c_n\cos\lambda_{bn}y+\mu\left(\sum_{m=0}^{\infty}\sum_{n=0}^{\infty}-B_{mn}\lambda_{bn}\sin\lambda_{bn}y+\xi'_{1b}(y)\sum_{m=0}^{\infty}e_m+\xi'_{2b}(y)\sum_{m=0}^{\infty}f_m\right) \tag{18}$$

and

$$K_{px0}\left(\sum_{m=0}^{\infty}\sum_{n=0}^{\infty}B_{mn}\cos\lambda_{bn}y+\xi_{1b}(y)\sum_{m=0}^{\infty}e_m+\xi_{2b}(y)\sum_{m=0}^{\infty}f_m\right)$$
$$=-\sum_{m=0}^{\infty}\sum_{n=0}^{\infty}A_{mn}\lambda_{bn}\sin\lambda_{bn}y+\xi'_{1b}(y)\sum_{m=0}^{\infty}a_m+\xi'_{2b}(y)\sum_{m=0}^{\infty}b_m+\sum_{n=0}^{\infty}g_n\cos\lambda_{bn}y. \tag{19}$$

In order to derive the constraint equations for the unknown Fourier coefficients, all the sine terms, and the polynomials and their derivatives in Eq. (18) will be expanded into Fourier cosine series. The related formulas are provided in Appendix A. By collecting the coefficients for the like cosine terms, one can eventually obtain the following equations:

$$-\overline{k}_{nx0}\beta_{1n}\sum_{m=0}^{\infty}a_m-\overline{k}_{nx0}\beta_{2n}\sum_{m=0}^{\infty}b_m+c_n+\mu\eta_{1n}\sum_{m=0}^{\infty}e_m+\mu\eta_{2n}\sum_{m=0}^{\infty}f_m$$
$$=\overline{k}_{nx0}\sum_{m=0}^{\infty}A_{mn}+\mu\sum_{m,q}B_{mq}\lambda_{bq}\kappa_{bn}^{q}\quad(n=0,1,2,\ldots). \tag{20}$$

Similarly, the substitution of Eqs. (12) and (13) into the remaining boundary conditions will lead to seven additional equations. Thus, a total of eight constraint equations can be derived as

$$a_m-K_{py0}\alpha_{1m}\sum_{n=0}^{\infty}c_n-K_{py0}\alpha_{2m}\sum_{n=0}^{\infty}d_n+\gamma_{1m}\sum_{n=0}^{\infty}g_n+\gamma_{2m}\sum_{n=0}^{\infty}h_n$$
$$=\sum_{n=0}^{\infty}K_{py0}A_{mn}+\sum_{p,n}B_{pn}\lambda_{ap}\tau_{am}^{p}\quad(m=0,1,2,\ldots), \tag{21}$$

$$b_m+K_{py1}\alpha_{1m}\sum_{n=0}^{\infty}(-1)^n c_n+K_{py1}\alpha_{2m}\sum_{n=0}^{\infty}(-1)^n d_n+\gamma_{1m}\sum_{n=0}^{\infty}(-1)^n g_n$$
$$+\gamma_{2m}\sum_{n=0}^{\infty}(-1)^n h_n=-K_{py1}\sum_{n=0}^{\infty}(-1)^n A_{mn}+\sum_{p,n}B_{pn}(-1)^n\lambda_{ap}\tau_{am}^{p}\quad(m=0,1,2,\ldots), \tag{22}$$

$$-\overline{k}_{nx0}\beta_{1n}\sum_{m=0}^{\infty}a_m-\overline{k}_{nx0}\beta_{2n}\sum_{m=0}^{\infty}b_m+c_n+\mu\eta_{1n}\sum_{m=0}^{\infty}e_m+\mu\eta_{2n}\sum_{m=0}^{\infty}f_m$$
$$=\overline{k}_{nx0}\sum_{m=0}^{\infty}A_{mn}+\mu\sum_{m,q}B_{mq}\lambda_{bq}\kappa_{bn}^{q}\quad(n=0,1,2,\ldots), \tag{23}$$

$$\overline{k}_{nx1}\beta_{1n}\sum_{m=0}^{\infty}(-1)^m a_m + \overline{k}_{nx1}\beta_{2n}\sum_{m=0}^{\infty}(-1)^m b_m + d_n + \mu\eta_{1n}\sum_{m=0}^{\infty}(-1)^m e_m + \mu\eta_{2n}\sum_{m=0}^{\infty}(-1)^m f_m$$
$$= -\overline{k}_{nx1}\sum_{m=0}^{\infty}(-1)^m A_{mn} + \mu\sum_{m,q} B_{mq}(-1)^m\lambda_{bq}\kappa_{bn}^{q} \quad (n = 0, 1, 2, \ldots), \tag{24}$$

$$\mu\gamma_{1m}\sum_{n=0}^{\infty} c_n + \mu\gamma_{2m}\sum_{n=0}^{\infty} d_n + e_m - \overline{k}_{ny0}\alpha_{1m}\sum_{n=0}^{\infty} g_n - \overline{k}_{ny0}\alpha_{2m}\sum_{n=0}^{\infty} h_n$$
$$= \mu\sum_{p,n} A_{pn}\lambda_{ap}\tau_{am}^{p} + \overline{k}_{ny0}\sum_{n=0}^{\infty} B_{mn} \quad (m = 0, 1, 2, \ldots), \tag{25}$$

$$\mu\gamma_{1m}\sum_{n=0}^{\infty}(-1)^n c_n + \mu\gamma_{2m}\sum_{n=0}^{\infty}(-1)^n d_n + f_m + \overline{k}_{ny1}\alpha_{1m}\sum_{n=0}^{\infty}(-1)^n g_n$$
$$+ \overline{k}_{ny1}\alpha_{2m}\sum_{n=0}^{\infty}(-1)^n h_n = \mu\sum_{p,n} A_{pn}(-1)^n\lambda_{ap}\tau_{am}^{p} - \overline{k}_{ny1}\sum_{n=0}^{\infty}(-1)^n B_{mn} \quad (m = 0, 1, 2, \ldots), \tag{26}$$

$$\eta_{1n}\sum_{m=0}^{\infty} a_m + \eta_{2n}\sum_{m=0}^{\infty} b_m - K_{px0}\beta_{1n}\sum_{m=0}^{\infty} e_m - K_{px0}\beta_{2n}\sum_{m=0}^{\infty} f_m + g_n$$
$$= \sum_{m,q} A_{mq}\lambda_{bq}\kappa_{bn}^{q} + K_{px0}\sum_{m=0}^{\infty} B_{mn} \quad (n = 0, 1, 2, \ldots), \tag{27}$$

$$\eta_{1n}\sum_{m=0}^{\infty}(-1)^m a_m + \eta_{2n}\sum_{m=0}^{\infty}(-1)^m b_m + K_{px1}\beta_{1n}\sum_{m=0}^{\infty}(-1)^m e_m + h_n + K_{px1}\beta_{2n}\sum_{m=0}^{\infty}(-1)^m f_m$$
$$= \sum_{m,q} A_{mq}(-1)^m\lambda_{bq}\kappa_{bn}^{q} - K_{px1}\sum_{m=0}^{\infty}(-1)^m B_{mn} \quad (n = 0, 1, 2, \ldots). \tag{28}$$

It is clear from the above equations that the expansion coefficients, a_m, b_m, c_n, d_n, e_m, f_m, g_n and h_n (m, $n = 0,1,2,\ldots$), in the single Fourier series are not independent unknowns; they are actually dependent upon the expansion coefficients, A_{mn} and B_{mn}, of the double Fourier series. When all the series expansions are truncated to $m = M$ and $n = N$ in numerical calculations, Eqs. (21)–(28) can be rewritten in matrix form as

$$\mathbf{HP} = \mathbf{QC}, \tag{29}$$

where

$$P = \{a_0, \ldots, a_M, b_0, \ldots, b_M, c_0, \ldots, c_N, d_0 \ldots, d_N, e_0 \ldots, e_M, f_0, \ldots, f_M, g_0, \ldots g_N, h_0, \ldots, h_N\}^{\mathrm{T}}, \tag{30}$$

$$\mathbf{C} = \begin{bmatrix} \mathbf{C}_1^{\mathrm{T}} & \mathbf{C}_2^{\mathrm{T}} \end{bmatrix}^{\mathrm{T}}, \tag{31}$$

$$\mathbf{C}_1 = \{A_{00}, A_{01}, \ldots, A_{m'0}, A_{m'1}, \ldots, A_{m'n'}, \ldots, A_{MN}\}^{\mathrm{T}}, \tag{32}$$

$$\mathbf{C}_2 = \{B_{00}, B_{01}, \ldots, B_{m'0}, B_{m'1}, \ldots, B_{m'n'}, \ldots, B_{MN}\}^{\mathrm{T}} \tag{33}$$

$$\mathbf{H}=\begin{bmatrix}\mathbf{a}_{11} & \mathbf{b}_{12} & \mathbf{c}_{13} & \mathbf{d}_{14} & \mathbf{e}_{15} & \mathbf{f}_{16} & \mathbf{g}_{17} & \mathbf{h}_{18}\\ \mathbf{a}_{21} & \mathbf{b}_{22} & \mathbf{c}_{23} & \mathbf{d}_{24} & \mathbf{e}_{25} & \mathbf{f}_{26} & \mathbf{g}_{27} & \mathbf{h}_{28}\\ \mathbf{a}_{31} & \mathbf{b}_{32} & \mathbf{c}_{33} & \mathbf{d}_{34} & \mathbf{e}_{35} & \mathbf{f}_{36} & \mathbf{g}_{37} & \mathbf{h}_{38}\\ \mathbf{a}_{41} & \mathbf{b}_{42} & \mathbf{c}_{43} & \mathbf{d}_{44} & \mathbf{e}_{45} & \mathbf{f}_{46} & \mathbf{g}_{47} & \mathbf{h}_{48}\\ \mathbf{a}_{51} & \mathbf{b}_{52} & \mathbf{c}_{53} & \mathbf{d}_{54} & \mathbf{e}_{55} & \mathbf{f}_{56} & \mathbf{g}_{57} & \mathbf{h}_{58}\\ \mathbf{a}_{61} & \mathbf{b}_{62} & \mathbf{c}_{63} & \mathbf{d}_{64} & \mathbf{e}_{65} & \mathbf{f}_{66} & \mathbf{g}_{67} & \mathbf{h}_{68}\\ \mathbf{a}_{71} & \mathbf{b}_{72} & \mathbf{c}_{73} & \mathbf{d}_{74} & \mathbf{e}_{75} & \mathbf{f}_{76} & \mathbf{g}_{77} & \mathbf{h}_{78}\\ \mathbf{a}_{81} & \mathbf{b}_{82} & \mathbf{c}_{83} & \mathbf{d}_{84} & \mathbf{e}_{85} & \mathbf{f}_{86} & \mathbf{g}_{87} & \mathbf{h}_{88}\end{bmatrix} \tag{34}$$

and

$$\mathbf{Q}=\begin{bmatrix}\mathbf{q}_{11}^{\mathrm{T}} & \mathbf{q}_{21}^{\mathrm{T}} & \mathbf{q}_{31}^{\mathrm{T}} & \mathbf{q}_{41}^{\mathrm{T}} & \mathbf{q}_{51}^{\mathrm{T}} & \mathbf{q}_{61}^{\mathrm{T}} & \mathbf{q}_{71}^{\mathrm{T}} & \mathbf{q}_{81}^{\mathrm{T}}\\ \mathbf{q}_{12}^{\mathrm{T}} & \mathbf{q}_{22}^{\mathrm{T}} & \mathbf{q}_{32}^{\mathrm{T}} & \mathbf{q}_{42}^{\mathrm{T}} & \mathbf{q}_{52}^{\mathrm{T}} & \mathbf{q}_{62}^{\mathrm{T}} & \mathbf{q}_{72}^{\mathrm{T}} & \mathbf{q}_{82}^{\mathrm{T}}\end{bmatrix}^{\mathrm{T}}. \tag{35}$$

The elements of the matrices **H** and **Q** can be directly determined from Eqs. (21)–(28), as demonstrated in Appendix B.

2.2. Solving the governing differential equations

The governing differential equations for the free in-plane vibration of a plate can be written as

$$\frac{\partial^2 u}{\partial x^2}+\frac{1}{2}(1-\mu)\frac{\partial^2 u}{\partial y^2}+\frac{1}{2}(1+\mu)\frac{\partial^2 v}{\partial x\,\partial y}+\frac{1}{c_L^2}\omega^2 u=0 \tag{36}$$

and

$$\frac{\partial^2 v}{\partial y^2}+\frac{1}{2}(1-\mu)\frac{\partial^2 v}{\partial x^2}+\frac{1}{2}(1+\mu)\frac{\partial^2 u}{\partial x\,\partial y}+\frac{1}{c_L^2}\omega^2 v=0, \tag{37}$$

where u and v are the displacements in the x- and y-direction, respectively, $c_L=\sqrt{E/\rho(1-\mu^2)}$ is the longitudinal wave speed in the plate, and ω is the angular frequency.

Substituting Eqs. (12) and (13) into (36) and (37) will lead to the following two equations:

$$\begin{aligned}
&-\sum_{m=0}^{\infty}\sum_{n=0}^{\infty}A_{mn}\lambda_{am}^2\cos\lambda_{am}x\cos\lambda_{bn}y+\xi_{1a}''(x)\sum_{n=0}^{\infty}c_n\cos\lambda_{bn}y+\xi_{2a}''(x)\sum_{n=0}^{\infty}d_n\cos\lambda_{bn}y\\
&-\xi_{1b}(y)\sum_{m=0}^{\infty}a_m\lambda_{am}^2\cos\lambda_{am}x-\xi_{2b}(y)\sum_{m=0}^{\infty}b_m\lambda_{am}^2\cos\lambda_{am}x\\
&+\frac{1-\mu}{2}\left[-\sum_{m=0}^{\infty}\sum_{n=0}^{\infty}A_{mn}\lambda_{bn}^2\cos\lambda_{am}x\cos\lambda_{bn}y+\xi_{1b}''(y)\sum_{m=0}^{\infty}a_m\cos\lambda_{am}x\right.\\
&\left.+\xi_{2b}''(y)\sum_{m=0}^{\infty}b_m\cos\lambda_{am}x-\xi_{1a}(x)\sum_{n=0}^{\infty}c_n\lambda_{bn}^2\cos\lambda_{bn}y-\xi_{2a}(x)\sum_{n=0}^{\infty}d_n\lambda_{bn}^2\cos\lambda_{bn}y\right]\\
&+\frac{1+\mu}{2}\left[\sum_{m=0}^{\infty}\sum_{n=0}^{\infty}B_{mn}\lambda_{am}\lambda_{bn}\sin\lambda_{am}x\sin\lambda_{bn}y-\xi_{1b}'(y)\sum_{m=0}^{\infty}e_m\lambda_{am}\sin\lambda_{am}x\right.\\
&\left.-\xi_{2b}'(y)\sum_{m=0}^{\infty}f_m\lambda_{am}\sin\lambda_{am}x-\xi_{1a}'(x)\sum_{n=0}^{\infty}g_n\lambda_{bn}\sin\lambda_{bn}y-\xi_{2a}'(x)\sum_{n=0}^{\infty}h_n\lambda_{bn}\sin\lambda_{bn}y\right]
\end{aligned}$$

$$+\frac{1}{c_L^2}\omega^2\left[\sum_{m=0}^{\infty}\sum_{n=0}^{\infty}A_{mn}\cos\lambda_{am}x\cos\lambda_{bn}y+\xi_{1b}(y)\sum_{m=0}^{\infty}a_m\cos\lambda_{am}x\right.$$
$$\left.+\xi_{2b}(y)\sum_{m=0}^{\infty}b_m\cos\lambda_{am}x+\xi_{1a}(x)\sum_{n=0}^{\infty}c_n\cos\lambda_{bn}y+\xi_{2a}(x)\sum_{n=0}^{\infty}d_n\cos\lambda_{bn}y\right]=0 \tag{38}$$

and

$$-\sum_{m=0}^{\infty}\sum_{n=0}^{\infty}B_{mn}\lambda_{bn}^2\cos\lambda_{am}x\cos\lambda_{bn}y+\xi_{1b}''(y)\sum_{m=0}^{\infty}e_m\cos\lambda_{am}x+\xi_{2b}''(y)\sum_{m=0}^{\infty}f_m\cos\lambda_{am}x$$
$$-\xi_{1a}(x)\sum_{n=0}^{\infty}g_n\lambda_{bn}^2\cos\lambda_{bn}y-\xi_{2a}(x)\sum_{n=0}^{\infty}h_n\lambda_{bn}^2\cos\lambda_{bn}y$$
$$+\frac{1-\mu}{2}\left[-\sum_{m=0}^{\infty}\sum_{n=0}^{\infty}B_{mn}\lambda_{am}^2\cos\lambda_{am}x\cos\lambda_{bn}y-\xi_{1b}(y)\sum_{m=0}^{\infty}e_m\lambda_{am}^2\cos\lambda_{am}x\right.$$
$$\left.-\xi_{2b}(y)\sum_{m=0}^{\infty}f_m\lambda_{am}^2\cos\lambda_{am}x+\xi_{1a}''(x)\sum_{n=0}^{\infty}g_n\cos\lambda_{bn}y+\xi_{2a}''(x)\sum_{n=0}^{\infty}h_n\cos\lambda_{bn}y\right]$$
$$+\frac{1+\mu}{2}\left[\sum_{m=0}^{\infty}\sum_{n=0}^{\infty}A_{mn}\lambda_{am}\lambda_{bn}\sin\lambda_{am}x\sin\lambda_{bn}y-\xi_{1b}'(y)\sum_{m=0}^{\infty}a_m\lambda_{am}\sin\lambda_{am}x\right.$$
$$\left.-\xi_{2b}'(y)\sum_{m=0}^{\infty}b_m\lambda_{am}\sin\lambda_{am}x-\xi_{1a}'(x)\sum_{n=0}^{\infty}c_n\lambda_{bn}\sin\lambda_{bn}y-\xi_{2a}'(x)\sum_{n=0}^{\infty}d_n\lambda_{bn}\sin\lambda_{bn}y\right]$$
$$+\frac{1}{c_L^2}\omega^2\left[\sum_{m=0}^{\infty}\sum_{n=0}^{\infty}B_{mn}\cos\lambda_{am}x\cos\lambda_{bn}y+\xi_{1b}(y)\sum_{m=0}^{\infty}e_m\cos\lambda_{am}x\right.$$
$$\left.+\xi_{2b}(y)\sum_{m=0}^{\infty}f_m\cos\lambda_{am}x+\xi_{1a}(x)\sum_{n=0}^{\infty}g_n\cos\lambda_{bn}y+\xi_{2a}(x)\sum_{n=0}^{\infty}h_n\cos\lambda_{bn}y\right]=0. \tag{39}$$

In order to solve for the unknown expansion coefficients, the polynomial and sine functions will all be expanded into Fourier cosine series. It needs to be pointed out that all the derivatives of the polynomials must be independently expanded into Fourier series, instead of taking a "short-cut" by differentiating the parent series expansions term-by-term. By doing such, Eqs. (38) and (39) can be finally reduced to

$$\left(\lambda_{am}^2+\frac{1-\mu}{2}\lambda_{bn}^2\right)A_{mn}+\left(\beta_{1n}\lambda_{am}^2-\frac{1-\mu}{2}\sigma_{1n}\right)a_m+\left(\beta_{2n}\lambda_{am}^2-\frac{1-\mu}{2}\sigma_{2n}\right)b_m$$
$$+\left(\frac{1-\mu}{2}\alpha_{1m}\lambda_{bn}^2-\varepsilon_{1m}\right)c_n+\left(\frac{1-\mu}{2}\alpha_{2m}\lambda_{bn}^2-\varepsilon_{2m}\right)d_n$$
$$-\frac{1+\mu}{2}\sum_p\sum_q B_{pq}\lambda_{ap}\lambda_{bq}\tau_{am}^p\kappa_{bn}^q$$
$$+\frac{1+\mu}{2}\sum_p e_p\eta_{1n}\lambda_{ap}\tau_{am}^p+\frac{1+\mu}{2}\sum_p f_p\eta_{2n}\lambda_{ap}\tau_{am}^p$$
$$+\frac{1+\mu}{2}\sum_q g_q\gamma_{1m}\lambda_{bq}\kappa_{bn}^q+\frac{1+\mu}{2}\sum_q h_q\gamma_{2m}\lambda_{bq}\kappa_{bn}^q$$
$$-\frac{1}{c_L^2}\omega^2(A_{mn}+a_m\beta_{1n}+b_m\beta_{2n}+\alpha_{1m}c_n+\alpha_{2m}d_n)=0 \tag{40}$$

and

$$\left(\lambda_{bn}^2+\frac{1-\mu}{2}\lambda_{am}^2\right)B_{mn}+\left(\frac{1-\mu}{2}\lambda_{am}^2\beta_{1n}-\sigma_{1n}\right)e_m+\left(\frac{1-\mu}{2}\lambda_{am}^2\beta_{2n}-\sigma_{2n}\right)f_m$$
$$+\left(\alpha_{1m}\lambda_{bn}^2-\frac{1-\mu}{2}\varepsilon_{1m}\right)g_n+\left(\alpha_{2m}\lambda_{bn}^2-\frac{1-\mu}{2}\varepsilon_{2m}\right)h_n$$
$$-\frac{1+\mu}{2}\sum_p\sum_q A_{pq}\lambda_{ap}\lambda_{bq}\tau_{am}^p\kappa_{bn}^q$$
$$+\frac{1+\mu}{2}\sum_p a_p\eta_{1n}\lambda_{ap}\tau_{am}^p+\frac{1+\mu}{2}\sum_p b_p\eta_{2n}\lambda_{ap}\tau_{am}^p$$
$$+\frac{1+\mu}{2}\sum_q c_q\gamma_{1m}\lambda_{bq}\kappa_{bn}^q+\frac{1+\mu}{2}\sum_q d_q\gamma_{2m}\lambda_{bq}\kappa_{bn}^q$$
$$-\frac{1}{c_L^2}\omega^2(B_{mn}+e_m\beta_{1n}+f_m\beta_{2n}+\alpha_{1m}g_n+\alpha_{2m}h_n)=0 \tag{41}$$

or, in matrix form

$$\begin{bmatrix}\mathbf{A}_{11} & \mathbf{A}_{12}\\ \mathbf{A}_{21} & \mathbf{A}_{22}\end{bmatrix}\mathbf{C}+\begin{bmatrix}\mathbf{B}_{11} & \mathbf{B}_{12}\\ \mathbf{B}_{21} & \mathbf{B}_{22}\end{bmatrix}\mathbf{P}-\frac{\omega^2}{c_L^2}\left\{\begin{bmatrix}\mathbf{E}_{11} & \mathbf{E}_{12}\\ \mathbf{E}_{21} & \mathbf{E}_{22}\end{bmatrix}\mathbf{C}+\begin{bmatrix}\mathbf{F}_{11} & \mathbf{F}_{12}\\ \mathbf{F}_{21} & \mathbf{F}_{22}\end{bmatrix}\mathbf{P}\right\}=0. \tag{42}$$

Representative expressions for these coefficient matrices can be found in Appendix B.

Making use of Eq. (29), the final system equations can be obtained as

$$\left(\mathbf{K}-\frac{\omega^2}{c_L^2}\mathbf{M}\right)\mathbf{C}=0, \tag{43}$$

where $\mathbf{K}=\mathbf{A}+\mathbf{B}\mathbf{H}^{-1}\mathbf{Q}$ and $\mathbf{M}=\mathbf{E}+\mathbf{F}\mathbf{H}^{-1}\mathbf{Q}$.

The natural frequencies and eigenvectors can now be easily and systematically determined from solving a standard matrix eigenproblem. Each of the eigenvectors actually contains the Fourier coefficients for the corresponding modes. The physical mode shapes can be simply obtained using Eqs. (12), (13) and (29). When the response to an applied excitation is desired, one needs to simply add a force term to the right-hand side of Eq. (43). Of course, the components of the force vector now represent the projections of the actual physical forces onto the Fourier functional space, a familiar procedure as used in the modal superposition method.

3. Results and discussions

Several examples involving different boundary conditions have been solved in this section. First, consider a plate clamped along all edges. A clamped edge for in-plane vibration can be viewed as a special case when the stiffnesses for the (normal and tangential) boundary springs become infinitely large which is actually represented by non-dimensional stiffness 4500 in the following numerical calculations. In Table 1, the first six non-dimensional frequency parameters, $\Omega=\omega a\sqrt{\rho(1-\mu^2)/E}$, are shown for the plates of various aspect ratios. The results compare very well with those obtained from the Rayleigh-Ritz energy method [9]. In the current calculations, both displacement expansions have been truncated equally to include only the first $(M+1)\times(N+1)$ terms corresponding to $m=0,1,2,\ldots,M$ and $n=0,1,2,\ldots,N$. However, it should be mentioned that in the cases where, for instance, involve plates with large aspect ratios, it may be more efficient to truncate the displacement expansions differently to account for the possibly different wave behaviors in the x- and y-direction. The frequency parameters given in Table 1 are calculated by setting $M=N=12$. To check the convergence of the solution, Table 2 shows the frequencies (for $b/a=1$) determined by using different numbers of the expansion terms, $M=N=4,5,6,7,8,9,10,11,12,13,14,15$. A desired convergence characteristic is observed in regards to: (a) sufficiently accurate results with only a small number of terms in the expansions,

Table 1
Frequency parameters, $\Omega = \omega a\sqrt{\rho(1-\mu^2)/E}$, for C-C-C-C plates of different aspect ratios

$r_1 = a/b$	$\Omega = \omega a\sqrt{\rho(1-\mu^2)/E}$					
	1	2	3	4	5	6
1.0	3.554 (3.555[a])	3.554 (3.555)	4.236 (4.235)	5.185 (5.186)	5.859 (5.859)	5.896 (5.895)
1.5	4.112	4.923	5.402	6.564	6.602	6.617
2.0	4.788 (4.789)	6.374 (6.379)	6.710 (6.712)	7.048 (7.049)	7.608 (7.608)	8.140 (8.140)
2.5	5.538	7.590	7.868	8.097	8.773	9.568
3.0	6.336	8.195	9.385	9.532	10.05	10.54

[a]Results in parentheses are taken from Ref. [9].

Table 2
Frequency parameters, $\Omega = \omega a\sqrt{\rho(1-\mu^2)/E}$, for a C-C-C-C square plate

$M = N$	$\Omega = \omega a\sqrt{\rho(1-\mu^2)/E}$					
	1	2	3	4	5	6
4	3.561	3.561	4.273	5.213	5.927	5.952
5	3.559	3.559	4.246	5.206	5.881	5.947
6	3.556	3.556	4.245	5.193	5.877	5.912
7	3.556	3.556	4.239	5.192	5.866	5.911
8	3.555	3.555	4.239	5.188	5.865	5.902
9	3.555	3.555	4.237	5.188	5.861	5.901
10	3.554	3.554	4.237	5.186	5.861	5.898
11	3.554	3.554	4.236	5.186	5.859	5.898
12	3.554	3.554	4.236	5.185	5.859	5.896
13	3.554	3.554	4.235	5.185	5.858	5.896
14	3.554	3.554	4.235	5.185	5.858	5.895
15	3.554	3.554	4.235	5.185	5.857	5.895

Table 3
Frequency parameters, $\Omega = \omega a\sqrt{\rho(1-\mu^2)/E}$, for F-F-F-F plates of different aspect ratios

$r_1 = a/b$	$\Omega = \omega a\sqrt{\rho(1-\mu^2)/E}$					
	1	2	3	4	5	6
1.0	2.321 (2.321[a])	2.472 (2.472)	2.472 (2.472)	2.629 (2.628)	2.988 (2.987)	3.452 (3.452)
1.5	2.197	2.881	2.915	3.938	3.971	4.380
2.0	1.954 (1.954)	2.961 (2.961)	3.268 (3.267)	4.725 (4.726)	4.785 (4.784)	5.205 (5.205)
2.5	1.747	2.976	3.337	4.969	5.169	5.683
3.0	1.571	2.983	3.224	4.951	5.754	5.830

[a]Results in parentheses are taken from Ref. [9].

and (b) a consistent improvement of the solution as more terms are included in the calculations (that is, the solution scheme is numerically stable). In view of the excellent numerical behavior of the current solution, the setting $M = N = 12$ will be used in all the subsequent calculations.

The next example is also about a classical case: a completely free plate. The free edge condition is equivalent to setting the stiffnesses for both the normal and tangential springs to zero. The six smallest frequency parameters, $\Omega = \omega a\sqrt{\rho(1-\mu^2)/E}$, are listed in Table 3 for various plate aspect ratios. The results from Ref. [9] are also shown there as a comparison. A good agreement is observed between these two sets of solutions.

Table 4
Natural frequencies of in-plane vibration of a rectangular plate with C-C-C-F boundary conditions

Mode no.	NASTRAN[a]	Present		Ref. [10]		Ref. [11]	
	Frequency (Hz)	Frequency (Hz)	Error (%)	Frequency (Hz)	Error (%)	Frequency (Hz)	Error (%)
1	1803	1802	0.06	1811	0.4	1892	4.9
2	2656	2657	0.04	2674	0.7	2727	2.7
3	2794	2800	0.21	2845	1.8	3026	8.4
4	3392	3402	0.29	3524	3.9	3596	6.0
5	3479	3492	0.37	3504	0.7	3624	4.2
6	3704	3730	0.70	3757	1.4	3868	4.4

[a]NASTRAN results are taken from Ref. [11].

Table 5
Natural frequencies of in-plane vibration of a rectangular plate with C-F-C-F boundary conditions

Mode no.	NASTRAN[a]	Present		Ref. [10]		Ref. [11]	
	Frequency (Hz)	Frequency (Hz)	Error (%)	Frequency (Hz)	Error (%)	Frequency (Hz)	Error (%)
1	1449	1445	0.28	1455	0.4	1531	7
2	2511	2514	0.12	2520	0.4	2682	6
3	2567	2566	0.04	2639	2.8	2697	5
4	2637	2642	0.19	2662	0.95	2994	12
5	3037	3037	0	3187	4.5	3122	3
6	3061	3073	0.39	3146	2.8	3390	10

[a]NASTRAN results are taken from Ref. [11].

Table 6
Frequency parameters, $\Omega = \omega a\sqrt{\rho(1-\mu^2)/E}$, for SS1-SS1-SS1-SS1 plates of different aspect ratios

$r_1 = a/b$	$\Omega = \omega a\sqrt{\rho(1-\mu^2)/E}$					
	1	2	3	4	5	6
1.0	1.858 (1.859[a])	1.858 (1.859)	2.629 (2.628)	3.718 (3.717)	3.718 (3.717)	4.157 (4.156)
1.5	1.858	2.787	3.351	3.718	4.647	5.576
2.0	1.858 (1.859)	3.716 (3.717)	3.718 (3.717)	4.155 (4.156)	5.258 (5.257)	5.577 (5.576)
2.5	1.858	3.717	4.645	5.003	5.577	5.951
3.0	1.858	3.717	5.573	5.577	5.875	6.701

[a]Results in parentheses are taken from Ref. [9].

Table 7
Frequency parameters, $\Omega = \omega a\sqrt{\rho(1-\mu^2)/E}$, for SS1-F-SS1-F plates of different aspect ratios

$r_2 = b/a$	$\Omega = \omega a\sqrt{\rho(1-\mu^2)/E}$					
	1	2	3	4	5	6
1.0	1.408	1.858	2.629	3.249	3.364	3.499
	(1.408[a])	–	–	(3.248)	(3.364)	(3.498)
1.25	1.487	1.497	2.313	2.974	3.194	3.223
	–	(1.497)	(2.312)	–	(3.194)	(3.222)
1.5	1.239	1.556	2.091	2.478	3.004	3.136
	–	(1.556)	(2.092)	–	(3.004)	(3.138)
2.0	0.929	1.624	1.858	1.866	2.629	2.788
	–	(1.624)	–	(1.866)	–	–

[a]Results in parentheses are taken from Ref. [6].

Next, consider two cases that involve the mixed combinations of the clamped and free edge conditions along the plate edges. These two types of problems are studied in Refs. [10,11]. In order to compare with their results, the model parameters including the plate aspect ratio and material properties are kept the same here. Plate dimensions are 1.0 m in length, 1.2 m in width, and 2.5 mm in thickness. Young's modulus is $E = 70 \times 10^9$ N/m^2 and density is

Table 8
Frequency parameters, $\Omega = \omega a\sqrt{\rho(1-\mu^2)/E}$, for SS1-C-SS1-C plates of different aspect ratios

$r_2 = b/a$	$\Omega = \omega a\sqrt{\rho(1-\mu^2)/E}$					
	1	2	3	4	5	6
1.0	1.858	3.275	3.494	3.718	4.411	4.957
	–	(3.276[a])	(3.494)	–	(4.410)	(4.958)
1.25	1.487	2.786	2.974	3.281	4.141	4.344
	–	(2.786)	–	(3.280)	(4.140)	(4.344)
1.5	1.239	2.479	2.500	3.122	3.719	3.943
	–	–	(2.500)	(3.122)	–	(3.944)
2.0	0.929	1.859	2.205	2.789	2.811	3.423
	–	–	(2.206)	–	(2.810)	(3.422)

[a]Results in parentheses are taken from Ref. [6].

Table 9
Frequency parameters, $\Omega = \omega a\sqrt{\rho(1-\mu^2)/E}$, for SS2-F-SS2-F plates of different aspect ratios

$r_2 = b/a$	$\Omega = \omega a\sqrt{\rho(1-\mu^2)/E}$					
	1	2	3	4	5	6
1.0	1.407	2.628	3.142	3.248	3.363	3.498
	(1.408[a])	–	–	–	(3.364)	(3.498)
1.25	1.497	2.313	2.513	3.192	3.222	3.318
	(1.497)	(2.312)	–	(3.194)	(3.222)	–
1.5	1.556	2.091	2.094	3.004	3.135	3.355
	(1.556)	–	(2.092)	(3.004)	(3.138)	–
2.0	1.571	1.624	1.866	2.628	3.059	3.142
	–	(1.624)	(1.866)	–	(3.060)	–

[a]Results in parentheses are taken from Ref. [6].

Table 10
Frequency parameters, $\Omega = \omega a\sqrt{\rho(1-\mu^2)/E}$, for SS2-C-SS2-C plates of different aspect ratios

$r_2 = b/a$	$\Omega = \omega a\sqrt{\rho(1-\mu^2)/E}$					
	1	2	3	4	5	6
1.0	3.140	3.275	3.494	4.411	4.957	5.622
	–	(3.276[a])	–	(4.410)	(4.958)	(5.622)
1.25	2.513	2.786	3.280	4.140	4.343	4.622
	–	(2.786)	–	(4.140)	(4.344)	–
1.5	2.094	2.500	3.121	3.943	3.999	4.014
	–	(2.500)	–	(3.944)	(3.998)	–
2.0	1.571	2.205	2.811	3.142	3.422	3.450
	–	(2.206)	–	–	(3.422)	–

[a]Results in parentheses are taken from Ref. [6].

$\rho = 2700\,\mathrm{kg/m^3}$, Poisson's ratio is $\mu = 0.33$. The corresponding modal frequencies are compared in Table 4 for the C-C-C-F plate, and in Table 5 for C-F-C-F plate. The FEM results calculated using NASTRAN are also given there. In both cases, the current solution matches better with the FEM data in comparison with other two solutions.

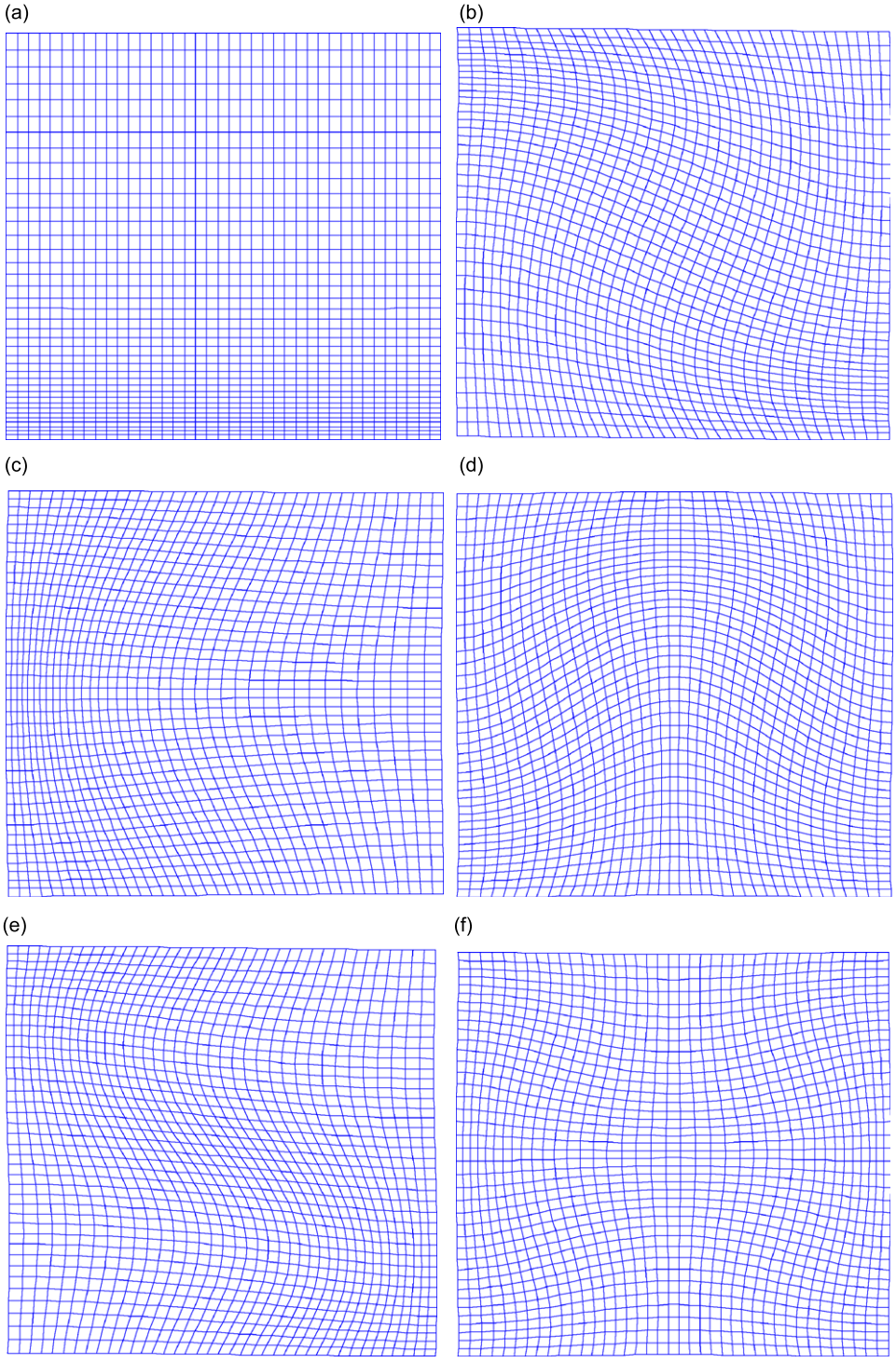

Fig. 2. The mode shapes for an SS2-C-SS2-C square plate: (a) the first mode; (b) second; (c) third; (d) fourth; (e) fifth; (f) sixth.

There exist two distinct types of 'simple support' boundary conditions for the in-plane vibration of a rectangular plate [6]. The first type of the simply supported condition specifies the zero displacement and zero force respectively in the directions parallel and normal to an edge, which is here described by setting the stiffnesses of the tangential and normal springs to ∞ and 0, respectively. The second type accounts for an exactly opposite scenario. For convenience, these two types of simply supported edge conditions are designated by SS1 and SS2. In Ref. [9], the simple support case actually refers to the first type.

The first six frequencies, $\Omega = \omega a\sqrt{\rho(1-\mu^2)/E}$, are given in Table 6 for simply supported plates of various aspect ratios. Similar results are presented in Tables 7 and 8 for plates with the mixed combinations of free, clamped and (the first type of) simply supported edges. To understand the difference between the SS1 and SS2 conditions, the problems associated with Tables 7 and 8 are re-solved by replacing the SS1 edges with SS2 while all the other parameters are kept the same. The results are presented in Tables 9 and 10. A comparison of these two sets results has revealed the significant difference between the SS1 and SS2 boundary conditions.

For any given modal frequency, the corresponding mode shape can be readily determined from Eqs. (12) and (13). As an example, the first six mode shapes are plotted in Fig. 2 for a square plate under SS2-C-SS2-C boundary conditions. It can be seen that although those are the lower-order modes, they are typically more complicated than their counterparts in the flexural vibrations; for instance, the extension-compression deformation in one region (or mode) can quickly turn into a shear state in another region (or mode). This characteristic, however, may have some favorable implications to the non-destructive evaluation of material and structural parameters and monitoring of structural conditions or failures, as evidenced by the more distinctively different modal signatures and more probing natures of the in-plane displacement fields. The complexity of mode shapes also graphically confirms the fact that the displacement fields can no longer be determined by the separation of variables for a plate under general boundary conditions.

Finally, consider a more complicated example in which an SS1-SS1-SS2-SS2 square plate is elastically restrained at $x = 0$ and $y = 0$ in the normal direction, and at $x = a$ and $y = b$ in the tangential direction; that is, $\bar{K}_{nx0} = \bar{K}_{ny0} = \bar{K}_{px1} = \bar{K}_{py1} = \bar{K}$ and all other restraining springs are set to have an infinite stiffness. For simplicity, all the restraining springs are assumed to have the same stiffness. The first six frequencies are presented in Table 11 for several different spring stiffness values. The FEM results calculated using ANSYS are also shown there as a comparison. For a very large stiffness value, this support condition will effectively degenerate to the familiar clamped condition, as evidenced by comparing the last row in Table 11 with the first row in Table 1. The mode shapes corresponding to $\bar{K} = 1$ are plotted in Fig. 3. The results clearly show that the normal springs at x and $y = 0$ have played a dominant role in these modes. In other words, one has to change the normal stiffness to effectively modify the modal properties.

4. Conclusions

A general analytical method has been developed for the in-plane vibration analysis of rectangular plates with elastically restrained edges. Each of the in-plane displacements is sought as a standard double Fourier

Table 11
Frequency parameters, $\Omega = \omega a\sqrt{\rho(1-\mu^2)/E}$, for an SS1-SS1-SS2-SS2 square plate with normal restraints at $x = 0$ and $y = 0$, and tangential restraints at $x = a$, $y = b$, that is, $\bar{K}_{nx0} = \bar{K}_{ny0} = \bar{K}_{px1} = \bar{K}_{py1} = \bar{K}$

$\bar{K}$	$\Omega = \omega a\sqrt{\rho(1-\mu^2)/E}$					
	1	2	3	4	5	6
0	1.314 (1.314[a])	2.221 (2.221)	2.939 (2.940)	2.939 (2.940)	3.943 (3.945)	4.739 (4.743)
0.5	1.856 (1.853)	2.533 (2.532)	3.226 (3.224)	3.272 (3.275)	4.159 (4.160)	4.918 (4.921)
1	2.175 (2.171)	2.702 (2.698)	3.428 (3.424)	3.555 (3.556)	4.324 (4.324)	5.044 (5.047)
1.5	2.395	2.814	3.572	3.779	4.460	5.139
2	2.557	2.897	3.676	3.956	4.576	5.216
∞	3.554	3.554	4.236	5.185	5.859	5.896

[a]Results in parentheses are calculated from ANSYS.

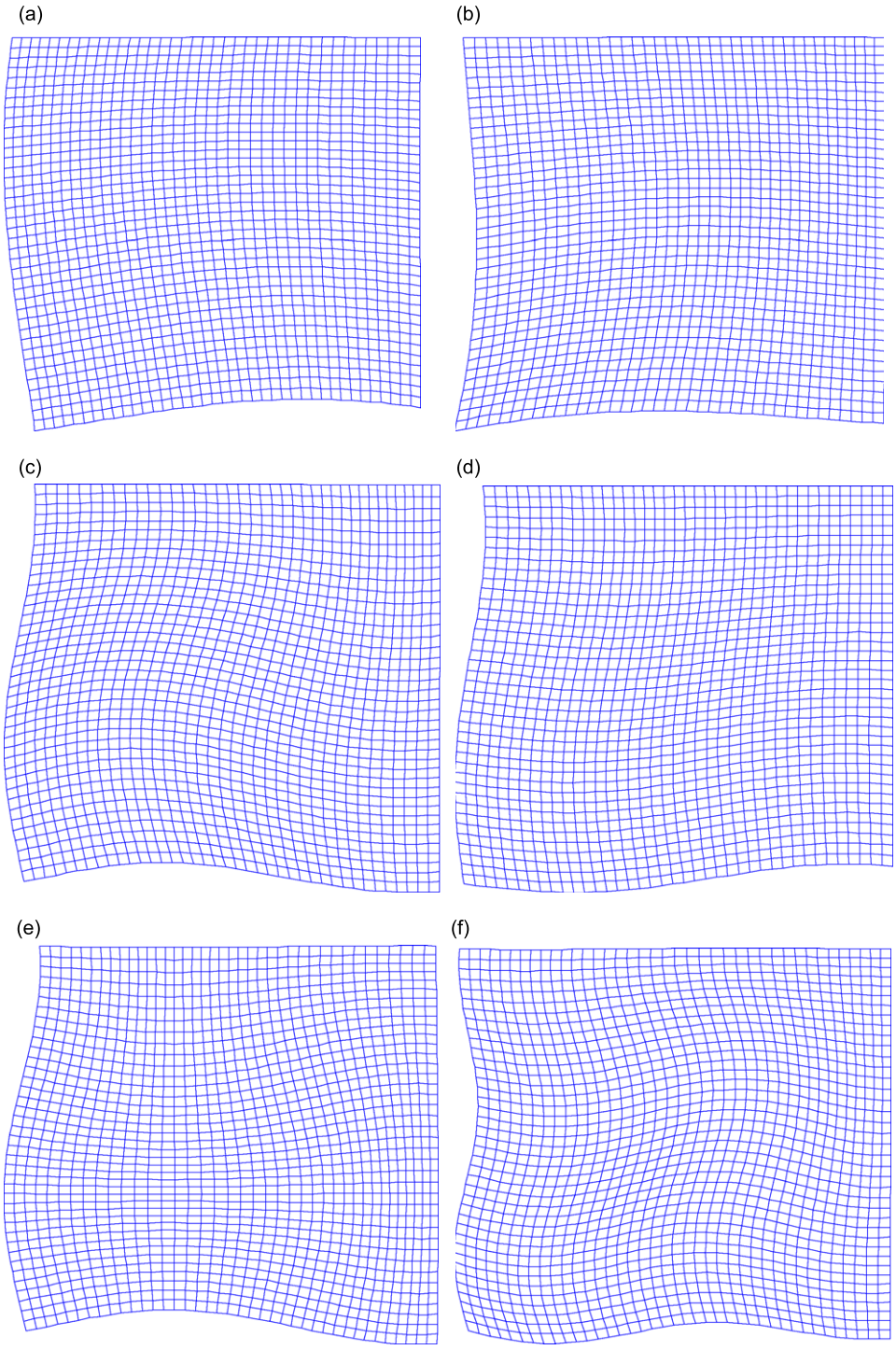

Fig. 3. The mode shapes for an SS1-SS1-SS2-SS2 square plate elastically restrained along $x = 0$, and $y = 0$ in the normal directions and along $x = a$, and $y = b$ in the tangential directions. $\bar{K} = 1$: (a) the first mode; (b) second; (c) third; (d) fourth; (e) fifth; (f) sixth.

cosine series expansion supplemented by four auxiliary functions in the form of the product of a polynomial and a single Fourier cosine series. These four auxiliary functions are introduced to deal with the potential discontinuities (or jumps) at the edges with the partial derivatives of the in-plane displacements

(or equivalently, the normal and shear forces). Although the polynomials are specifically used in the current derivations, any other closed-form functions should work as well provided they have continuous first-order derivatives. Unlike most methods in which each of the frequency parameters has to be sought repeatedly and iteratively from a highly nonlinear characteristic equation, all the modal parameters can now be easily determined from solving a standard matrix eigenproblem. The excellent accuracy and convergence of the present solution have been demonstrated through numerical examples. Of equal importance, this method has provided a unified solution to the in-plane vibration problems in that: for different boundary conditions, (a) the modal properties can readily be obtained by simply varying the stiffnesses of the restraining springs accordingly and (b) the dynamic response to an applied load can be determined using an invariant set of basis functions, which may be of importance to many applications such as fault detection and system identification. Finally, to the best of authors' knowledge this study appears to be the first time that an analytical solution is derived for the in-plane vibrations of rectangular plates with elastically restrained edges.

Acknowledgements

The second author gratefully acknowledges the financial support from NSF Grant CMS-0528263 under the supervision of Dr. Eduardo Misawa.

Appendix A. Supplementary definition

$$\xi_{1a}(x) = a\zeta_x(\zeta_x - 1)^2 = \sum_{m=0}^{\infty} \alpha_{1m} \cos \lambda_{am} x, \tag{A.1}$$

$$\alpha_{1m} = \begin{cases} \dfrac{a}{12}, & m = 0, \\ -\dfrac{2a\left[m^2\pi^2 - 6 + 6(-1)^m\right]}{m^4\pi^4}, & m \neq 0, \end{cases}$$

$$\xi'_{1a}(x) = \left(\frac{x}{a} - 1\right)^2 + \frac{2x}{a}\left(\frac{x}{a} - 1\right) = \sum_{m=0}^{\infty} \gamma_{1m} \cos \lambda_{am} x, \tag{A.2}$$

$$\gamma_{1m} = \begin{cases} 0, & m = 0, \\ \dfrac{4[2 + (-1)^m]}{m^2\pi^2}, & m \neq 0, \end{cases}$$

$$\xi''_{1a}(x) = \frac{4}{a}\left(\frac{x}{a} - 1\right) + \frac{2x}{a^2} = \sum_{m=0}^{\infty} \varepsilon_{1m} \cos \lambda_{am} x, \tag{A.3}$$

$$\varepsilon_{1m} = \begin{cases} -\dfrac{1}{a}, & m = 0, \\ \dfrac{12[-1 + (-1)^m]}{am^2\pi^2}, & m \neq 0, \end{cases}$$

$$\xi_{2a}(x) = \frac{1}{a}x^2\left(\frac{x}{a} - 1\right) = \sum_{m=0}^{\infty} \alpha_{2m} \cos \lambda_{am} x, \tag{A.4}$$

$$\alpha_{2m} = \begin{cases} -\dfrac{a}{12}, & m = 0, \\ \dfrac{2a\left[m^2\pi^2(-1)^m + 6 - 6(-1)^m\right]}{m^4\pi^4}, & m \neq 0, \end{cases}$$

$$\xi'_{2a}(x) = \frac{2}{a}x\left(\frac{x}{a} - 1\right) + \frac{x^2}{a^2} = \sum_{m=0}^{\infty} \gamma_{2m} \cos \lambda_{am} x, \tag{A.5}$$

$$\gamma_{2m} = \begin{cases} 0, & m = 0, \\ \dfrac{4[1 + 2(-1)^m]}{m^2\pi^2}, & m \neq 0, \end{cases}$$

$$\xi''_{2a}(x) = \frac{2}{a}\left(\frac{x}{a} - 1\right) + \frac{4x}{a^2} = \sum_{m=0}^{\infty} \varepsilon_{2m} \cos \lambda_{am} x, \tag{A.6}$$

$$\varepsilon_{2m} = \begin{cases} \dfrac{1}{a}, & m = 0, \\ \dfrac{12[-1 + (-1)^m]}{am^2\pi^2}, & m \neq 0, \end{cases}$$

$$\xi_{1b}(y) = y\left(\frac{y}{b} - 1\right)^2 = \sum_{n=0}^{\infty} \beta_{1n} \cos \lambda_{bn} y, \tag{A.7}$$

$$\beta_{1n} = \begin{cases} \dfrac{b}{12}, & n = 0, \\ -\dfrac{2b\left[n^2\pi^2 - 6 + 6(-1)^n\right]}{n^4\pi^4}, & n \neq 0, \end{cases}$$

$$\xi'_{1b}(y) = \left(\frac{y}{b} - 1\right)^2 + 2\frac{y}{b}\left(\frac{y}{b} - 1\right) = \sum_{n=0}^{\infty} \eta_{1n} \cos \lambda_{bn} y, \tag{A.8}$$

$$\eta_{1n} = \begin{cases} 0, & n = 0, \\ \dfrac{4[2 + (-1)^n]}{n^2\pi^2}, & n \neq 0, \end{cases}$$

$$\xi''_{1b}(y) = \frac{4}{b}\left(\frac{y}{b} - 1\right) + \frac{2y}{b^2} = \sum_{n=0}^{\infty} \sigma_{1n} \cos \lambda_{bn} y, \tag{A.9}$$

$$\sigma_{1n} = \begin{cases} -\dfrac{1}{b}, & n = 0, \\ \dfrac{12[-1 + (-1)^n]}{bn^2\pi^2}, & n \neq 0, \end{cases}$$

$$\xi_{2b}(y) = \frac{1}{b}y^2\left(\frac{y}{b} - 1\right) = \sum_{n=0}^{\infty} \beta_{2n} \cos \lambda_{bn} y, \tag{A.10}$$

$$\beta_{2n} = \begin{cases} -\dfrac{b}{12}, & n = 0, \\ \dfrac{2b\left[n^2\pi^2(-1)^n + 6 - 6(-1)^n\right]}{n^4\pi^4}, & n \neq 0, \end{cases}$$

$$\xi'_{2b}(y) = 2\frac{y}{b}\left(\frac{y}{b} - 1\right) + \frac{y^2}{b^2} = \sum_{n=0}^{\infty} \eta_{2n} \cos \lambda_{bn} y, \tag{A.11}$$

$$\eta_{2n} = \begin{cases} 0, & n = 0, \\ \dfrac{4[1 + 2(-1)^n]}{n^2\pi^2}, & n \neq 0, \end{cases}$$

$$\xi''_{2b}(y) = \frac{2}{b}\left(\frac{y}{b} - 1\right) + \frac{4y}{b^2} = \sum_{n=0}^{\infty} \sigma_{2n} \cos \lambda_{bn} y, \tag{A.12}$$

$$\sigma_{2n} = \begin{cases} \dfrac{1}{b}, & n = 0, \\ \dfrac{12[-1 + (-1)^n]}{bn^2\pi^2}, & n \neq 0, \end{cases}$$

$$\sin \lambda_{am} x = \sum_p \tau_{ap}^m \cos \lambda_{ap} x = \sin \lambda_{ap} x = \sum_m \tau_{am}^p \cos \lambda_{am} x, \tag{A.13}$$

$$p = 0, \quad \tau_{am}^p = 0,$$

$$p \neq 0, \quad \tau_{am}^p = \begin{cases} m = 0, & \dfrac{1 - (-1)^p}{p\pi}, \\ m \neq 0, & \begin{cases} m = p, & 0, \\ m \neq p, & \dfrac{2p\left[(-1)^{m+p} - 1\right]}{(m^2 - p^2)\pi}, \end{cases} \end{cases}$$

$$\sin \lambda_{bn} y = \sum_q \kappa_{bq}^n \cos \lambda_{bq} y = \sin \lambda_{bq} y = \sum_n \kappa_{bn}^q \cos \lambda_{bn} y, \tag{A.14}$$

$$q = 0, \quad \kappa_{bn}^q = 0,$$

$$q \neq 0, \quad \kappa_{bn}^q = \begin{cases} n = 0, & \dfrac{1 - (-1)^q}{q\pi}, \\ n \neq 0, & \begin{cases} n = q, & 0, \\ n \neq q, & \dfrac{2q\left[(-1)^{n+q} - 1\right]}{(n^2 - q^2)\pi}. \end{cases} \end{cases}$$

Appendix B. Additional definitions

To show the structures of the coefficient matrices in Eqs. (34) and (35), the elements which are derived from the $(m+1)$th equation of Eq. (21) are given below:

$$\text{for } m' = 0, 1, 2, \ldots, M, \;\; n' = 0, 1, 2, \ldots, N,$$

$$\{\mathbf{a}_{11}\}_{m+1,m'+1} = \delta_{mm'}, \quad \{\mathbf{b}_{12}\}_{m+1,m'+1} = 0, \tag{B.1,B.2}$$

$$\{\mathbf{c}_{13}\}_{m+1,n'+1} = -K_{py0}\alpha_{1m}, \quad \{\mathbf{d}_{14}\}_{m+1,n'+1} = -K_{py0}\alpha_{2m}, \tag{B.3,B.4}$$

$$\{\mathbf{e}_{15}\}_{m+1,m'+1} = 0, \quad \{\mathbf{f}_{16}\}_{m+1,m'+1} = 0, \tag{B.5,B.6}$$

$$\{\mathbf{g}_{17}\}_{m+1,n'+1} = \gamma_{1m}, \quad \{\mathbf{h}_{18}\}_{m+1,n'+1} = \gamma_{2m}. \tag{B.7,B.8}$$

Two new indices, $s = m(N+1)+n+1$ and $t = m'(N+1)+n'+1$, are defined here to simplify the following notations:

$$\{\mathbf{q}_{11}\}_{m+1,t} = K_{py0}\delta_{mm'}, \quad \{\mathbf{q}_{12}\}_{m+1,t} = \lambda_{am'}\tau_{am}^{m'}. \tag{B.9,B.10}$$

The elements of the coefficient matrices in Eq. (42) which correspond to the sth equation of Eq. (40) can be expressed as

$$\{\mathbf{A}_{11}\}_{s,t} = \left(\lambda_{am}^2 + \frac{1-\mu}{2}\lambda_{bn}^2\right)\delta_{st}, \quad \{\mathbf{A}_{12}\}_{s,t} = -\frac{1+\mu}{2}\lambda_{am'}\lambda_{bn'}\tau_{am}^{m'}\kappa_{bn}^{n'}, \tag{B.11,B.12}$$

$$\{\mathbf{B}_{11-\mathbf{a}}\}_{s,m'+1} = \left(\beta_{1n}\lambda_{am}^2 - \frac{1-\mu}{2}\sigma_{1n}\right)\delta_{mm'}, \tag{B.13}$$

$$\{\mathbf{B}_{11-\mathbf{b}}\}_{s,m'+1} = \left(\beta_{2n}\lambda_{am}^2 - \frac{1-\mu}{2}\sigma_{2n}\right)\delta_{mm'}, \tag{B.14}$$

$$\{\mathbf{B}_{11-\mathbf{c}}\}_{s,n'+1} = \left(\frac{1-\mu}{2}\alpha_{1m}\lambda_{bn}^2 - \varepsilon_{1m}\right)\delta_{nn'}, \tag{B.15}$$

$$\{\mathbf{B}_{11-\mathbf{d}}\}_{s,n'+1} = \left(\frac{1-\mu}{2}\alpha_{2m}\lambda_{bn}^2 - \varepsilon_{2m}\right)\delta_{nn'}, \tag{B.16}$$

$$\{\mathbf{B}_{12-\mathbf{e}}\}_{s,m'+1} = \frac{1+\mu}{2}\eta_{1n}\lambda_{am'}\tau_{am}^{m'}, \tag{B.17}$$

$$\{\mathbf{B}_{12-\mathbf{f}}\}_{s,m'+1} = \frac{1+\mu}{2}\eta_{2n}\lambda_{am'}\tau_{am}^{m'}, \tag{B.18}$$

$$\{\mathbf{B}_{12-\mathbf{g}}\}_{s,n'+1} = \frac{1+\mu}{2}\gamma_{1m}\lambda_{bn'}\kappa_{bn}^{n'}, \tag{B.19}$$

$$\{\mathbf{B}_{12-\mathbf{h}}\}_{s,n'+1} = \frac{1+\mu}{2}\gamma_{2m}\lambda_{bn'}\kappa_{bn}^{n'}, \tag{B.20}$$

$$\{\mathbf{E}_{11}\}_{s,t} = \delta_{st}, \quad \{\mathbf{E}_{12}\}_{s,t} = 0, \tag{B.21,B.22}$$

$$\{\mathbf{F}_{11-\mathbf{a}}\}_{s,m'+1} = \beta_{1n}\delta_{mm'}, \quad \{\mathbf{F}_{11-\mathbf{b}}\}_{s,m'+1} = \beta_{2n}\delta_{mm'}, \tag{B.23,B.24}$$

$$\{\mathbf{F}_{11-\mathbf{c}}\}_{s,n'+1} = \alpha_{1m}\delta_{nn'}, \quad \{\mathbf{F}_{11-\mathbf{d}}\}_{s,n'+1} = \alpha_{2m}\delta_{nn'}, \tag{B.25,B.26}$$

$$\{\mathbf{F}_{12-\mathbf{e}}\}_{s,m'+1} = 0, \quad \{\mathbf{F}_{12-\mathbf{f}}\}_{s,m'+1} = 0, \tag{B.27,B.28}$$

$$\{\mathbf{F}_{12-\mathbf{g}}\}_{s,n'+1} = 0, \quad \{\mathbf{F}_{12-\mathbf{h}}\}_{s,n'+1} = 0. \tag{B.29,B.30}$$

References

[1] A.N. Bercin, An assessment of the effects of in-plane vibrations on the energy flow between coupled plates, *Journal of Sound and Vibration* 191 (1996) 661–680.
[2] A.W. Leissa, *Vibration of plates*, Acoustical Society of America, 1993.
[3] A.W. Leissa, The free vibration of rectangular plates, *Journal of Sound and Vibration* 31 (1973) 257–293.
[4] R.H. Lyon, In-plane contribution to structural noise transmission, *Noise Control Engineering Journal* 26 (1985) 22–27.
[5] R.S. Langley, A.N. Bercin, Wave intensity analysis of high frequency vibrations, *Philosophical Transactions of the Royal Society of London A* 346 (1994) 489–499.
[6] D.J. Gorman, Exact solutions for the free in-plane vibration of rectangular plates with two opposite edges simply supported, *Journal of Sound and Vibration* 294 (2006) 131–161.
[7] W.L. Li, Free vibrations of beams with general boundary conditions, *Journal of Sound and Vibration* 237 (2000) 709–725.
[8] W.L. Li, Vibration analysis of rectangular plates with general elastic boundary supports, *Journal of Sound and Vibration* 273 (2004) 619–635.
[9] N.S. Bardell, R.S. Langley, J.M. Dunsdon, On the free in-plane vibration of isotropic rectangular plates, *Journal of Sound and Vibration* 191 (1996) 459–467.
[10] G. Wang, N.M. Wereley, Free in-plane vibration of rectangular plates, *AIAA Journal* 40 (2002) 953–959.
[11] N.H. Farag, J. Pan, Modal characteristics of in-plane vibration of rectangular plates, *Journal of the Acoustical Society of America* 105 (1999) 3295–3310.